Hydrogen Bonding and Proton Transfer in the Ground and Lowest Excited Singlet States of o-Hydroxyacetophenone

ARTICLE *in* THE JOURNAL OF PHYSICAL CHEMISTRY · JANUARY 1995

Impact Factor: 2.78 · DOI: 10.1021/j100002a031 · Source: OAI

2 AUTHORS:

Mikhail V Vener
Mendeleev Russian University of Chemical Te…
69 PUBLICATIONS **1,185** CITATIONS
SEE PROFILE

Steve Scheiner
Utah State University
366 PUBLICATIONS **11,154** CITATIONS
SEE PROFILE

Hydrogen Bonding and Proton Transfer in the Ground and Lowest Excited Singlet States of *o*-Hydroxyacetophenone

M. V. Vener and Steve Scheiner*

Department of Chemistry, Southern Illinois University, Carbondale, Illinois 62901

Received: August 12, 1994; In Final Form: October 25, 1994[⊗]

The potential energy surface of the ground state and lowest lying singlet of *o*-hydroxyacetophenone was calculated at the *ab initio* SCF and CIS levels, respectively, using a split-valence basis set to which was added polarization functions on atoms involved in the intramolecular H-bond. Whereas these potentials each contain one minimum corresponding to the normal form and a second well for the proton-transferred tautomer, only one minimum appears in these potentials after correlation is added. $S_0 \rightarrow S_1$ excitation hence induces the tautomerization associated with intramolecular proton transfer from the hydroxyl to the carbonyl oxygen. The excited state proton transfer may involve a nonradiative transition from the $S_1(n\pi^*)$ state to $S_1(\pi\pi^*)$. The vibrational spectra of the two tautomers have certain strong differences. Anharmonic adiabatic treatment of the OH···O segment of the molecule leads to improved reproduction of experimentally observed ν(O···O) and ν(OH) frequencies.

Introduction

Structures and dynamic processes in the excited states of salicylic acid and related molecules have been studied extensively in recent years.[1-3] One factor that makes this family particularly interesting is that they are the simplest among aromatic molecules containing an intramolecular asymmetric OH···O H-bond. The spectroscopy has demonstrated that excited state proton transfer (ESPT) can take place very rapidly and that there is a complex interplay between various accessible states. Understanding the specific mechanisms involved in ESPT in these comparatively simple molecules can lead to valuable insights into the behavior of larger systems.

Detailed understanding of the transfer in any electronic state requires knowledge of an extensive region of the pertinent PES. In this sense, *o*-hydroxyacetophenone (OHAP) has some essential advantages over other derivatives of salicylic acid. In contrast to methyl salicylate,[4] OHAP has no rotamers in the S_0 state. OHAP is photochemically stable in the S_1 state, unlike *o*-hydroxybenzaldehyde[5] and cannot exist in the form of self-associated dimers, like salicylic acid itself.[3]

With specific regard to OHAP, there remain a number of uncertainties about the structure of the excited state tautomer[1] and the exact nature of the lowest excited singlet state (cf. refs 6 and 7). Moreover, the distortion of the excited state potential energy surface (PES) with respect to that of the ground state has made vibrational assignment of the excitation spectra particularly problematic.[8] In order to aid in clarification of these issues, theoretical methods are applied here. The PES of each of the two states of interest are computed by *ab initio* methods. Vibrational analysis is carried out first within the harmonic approximation, followed by application of the localized OH···O fragment model[9] which includes anharmonic effects.

Methods of Calculation

A. *Ab Initio* Calculations. The equilibrium geometries and vibrational spectrum of OHAP in its S_0 and S_1 electronic states were computed at the *ab initio* SCF and CIS[10] levels, respectively. The calculations were performed using the Gaussian 92 package.[11] The basis set was based upon the 6-31G[12] type: p-type polarization functions (α = 1.10) were added to the bridging H atom and d-type functions (α = 0.80) to O. The atomic numbering scheme is presented in Figure 1, along with the structures of the primary and tautomeric forms. The distance of the bridging H_6 to the O_5 atom is designated as r, while R represents the interoxygen distance of the H-bond. A potential energy surface was constructed by first designating a two-dimensional grid of specific values of r and R. For each point on this grid, all remaining geometrical degrees of freedom were fully optimized. Electron correlation was incorporated into the ground and excited state PES computations via a second-order Moller-Plesset correction to either the SCF or CIS energy.

B. Dynamics Calculations. There are two principal approaches to the theoretical study of proton transfer in H-bonded systems containing the AH···B fragment. The reaction surface Hamiltonian method[13,14] treats the reaction pathway in terms of simultaneous and complex movements of the entire molecular frame. The second approach makes the approximation that the proton motion can be essentially decoupled from distant geometry changes, so that the reaction can be described in terms of the localized AH···B fragment.[9] More details of the application of these methods to the study of proton transfer (PT) in H-bonded systems can be found elsewhere.[15]

Consider the nonlinear H-bonded triatomic fragment A-H···B, with masses M_A, M_H, and M_B, where M_A (M_B) $\gg M_H$. The A-H and A···B interatomic distances are designated respectively as r and R, and the B···A-H angle by θ. A simplified Hamiltonian can be written as[15]

$$H = -\frac{\hbar^2}{2m^*}\frac{\partial^2}{\partial r^2} - \frac{\hbar^2}{2m^* r^2}\frac{\partial^2}{\partial \theta^2} - \frac{\hbar^2}{2M}\frac{\partial^2}{\partial R^2} + \mathrm{PES}(r,\theta,R) \quad (1)$$

where PES(r,θ,R) is a three-dimensional potential energy surface in a given electronic state. The reduced masses are

$$m^* = M_H M_A/(M_H + M_A) \quad (2a)$$

for the proton motion, and

$$M = M_B\,(M_A + M_H)/(M_B + M_A + M_H) \quad (2b)$$

for the heavy particles.

[⊗] Abstract published in *Advance ACS Abstracts*, December 15, 1994.

0022-3654/95/2099-0642$09.00/0

It was shown in ref 15 that the bending vibration plays only a minor role in modulation of the PT potential in the S_0 and S_1 electronic states of tropolone, and it can be neglected in the vibrational frequencies calculations. We assume that this is true for OHAP as well, and the bending coordinate is consequently relegated to the group of other degrees of freedom, fully optimized in the PES calculation. The two-dimensional stretching model, used in the present paper for the description of PT in the ground and first excited singlet state of OHAP, agrees with the implications of the recent femtosecond studies of ESPT in 2-(2-hydroxyphenyl)benzothiazole[16] and methylsalicylate.[17] According to these works, the ESPT in these compounds results from coupling between the O−H stretch and some low-frequency coordinate.

Making the above assumption, one can write the wave equation for PT in the 2-D PES as

$$\left\{-\frac{\hbar^2}{2m^*}\frac{\partial^2}{\partial r^2}-\frac{\hbar^2}{2M}\frac{\partial^2}{\partial R^2}+\mathrm{PES}(r,R)-E\right\}\Phi_{vn}(r,R)=0 \quad (3)$$

The applicability of the adiabatic separation of vibrational coordinates has been convincingly demonstrated in a series of papers.[18-29] Accordingly, separation of the r and R variables leads to the following form of the complete nuclear wave function:

$$\Phi_{vn}(r,R)=\phi_v(r,R)\,\chi_{vn}(R) \quad (4)$$

where v and n represent the vibrational quantum numbers corresponding respectively to the H or D stretching mode (variable r, "fast" subsystem) and the O···O stretching mode (variable R, "slow" subsystem).

Following refs 29−31 we assume that the PES(r,R) in eq 3 depends on R as a parameter and may hence be written as

$$\mathrm{PES}(r,R)=V(r,R)+W(R) \quad (5)$$

where $V(r,R)$ is an adiabatic potential for the "fast" subsystem and $W(R)$ is the O···O interaction energy.

Using eqs 4 and 5, the wave equation for H (D) stretching can be written as

$$H_1\phi_v(r,R)=\mathbf{e}_v(R)\,\phi_v(r,R) \quad (6)$$

where

$$H_1=-\frac{\hbar^2}{2m^*}\frac{\partial^2}{\partial r^2}+V(r,R)$$

The $V(r,R)$ function was fit to polynomials of sixth or eighth power of r at different values of R. The result is a family of adiabatic curves $\mathbf{e}_v(R)$ which describe the proton (deuteron) adiabatic energy as a function of R. Using eqs 5 and 6 the potential energy of the O···O stretching vibrations, associated with the vth proton (deuteron) state, can be written as

$$\epsilon_V(R)=\mathbf{e}_v(R)+W(R) \quad (7)$$

$\epsilon_V(R)$ functions were approximated by polynomials of fourth order.

The wave equation that remains to be solved for the O···O stretching vibrations is

$$H_2\chi_{vn}(R)=E_{vn}\chi_{vn}(R) \quad (8)$$

where

$$H_2=-\frac{\hbar^2}{2M}\frac{\partial^2}{\partial R^2}+\epsilon_V(R)$$

Vibrational eigenstates were computed using numerical methods described in ref 32 (eq 6) and the renormalized Numerov method[33] (eq 8).

Results

A. Geometries and Energetics. The equilibrium geometries of OHAP in the ground state were fully optimized at the SCF level of theory. The results are presented in Table 1, together with the available experimental values, using atomic labeling defined in Figure 1. This structure will be denoted the primary form. Comparison of the first column with the next two columns of data in Table 1 illustrates the good agreement of calculated geometries with the experiment, both gas phase and in the crystal. Of greatest import here are the aspects of the H-bond geometry. The interoxygen distance is reproduced very well, and the discrepancy in the O···OH angle is only 3.5°.

The tautomeric form, resulting from a proton transfer, was found to be higher in energy than the normal form by 17.7 kcal/mol in the S_0 state. The tautomer corresponds to a second (local) minima on the ground state PES. As one progresses around the OCCCO H-chelate ring, the "single" bonds become shorter and the "double" bonds longer in the tautomer as compared to the primary form. As can be seen by comparison of the appropriate columns of Table 1, the tautomer has a shortened interoxygen distance, compared to the primary form, and a closer placement of the bridging hydrogen to the O···O axis. The tautomer can hence be treated as a metastable state in S_0, in accord with previous theoretical[1,34a] data.

One explanation for the higher energy of the tautomer might be the loss of some aromaticity in the benzene ring, as suggested by Sobolewski and Domcke[34a] for a related molecule. Another perspective concerns the sort of system to which the OH group is attached. The primary form connects −OH to the benzene ring in a phenol-like arrangement, known to be quite stable. In contrast, the hydroxyl is attached to a double bond in the tautomer, forming a relatively unstable enol moiety.

Turning now to the S_1 state, the tautomeric form was found to be the most stable structure. A similar reversal in stability between the primary and tautomeric forms upon excitation has been predicted by semiempirical[37,38] and *ab initio*[34a,39,40] calculations of various molecules, as well as interpretation of experimental data.[57,58] Interpretations have been provided based on proton affinities[40] and/or acidity[41] of the H-bonded atoms. The energy of the primary form was found here to be only 0.8 kcal/mol higher than that of the tautomer, discrepant from expectations based on experiment.[8] Incorporation of electron correlation into the computations via MP2 yielded much improved agreement, as detailed in section C below. The fully optimized CIS geometry of the tautomeric form is presented in the fourth column of Table 1. Comparison with the first column highlights the drastic changes of geometric parameters of the H-chelate ring that accompany the $S_1 \leftarrow S_0$ excitation. Of particular interest, the hydroxyl C−O bond of the primary form takes on carbonyl character and vice versa for C_2O_1, in accord with experimental data.[8] Of greatest import here again are the aspects of the H-bond geometry. Calculations reveal a 0.07 Å contraction of the O···O equilibrium distance upon excitation. Such a reduction can be responsible for the appearance of low-frequency mode progressions, associated with the O···O stretching vibrations, observed in the experiments.[8] In contrast to the behavior of the H-chelate ring, the benzene ring is relatively unaffected by the excitation. Our results indicate the tautomer

TABLE 1: Total Energy (hartrees), Bond lengths (Å), and Angles (deg) of Stable Tautomers of OHAP in the S_0 and S_1 Electronic States, Obtained Using SCF and CIS Methods, Respectively

	S_0				S_1
	(primary form)[a]	microwave[b]	crystal[c]	(tautomer)	(tautomer)[d]
			Bond Lengths		
O···O	2.622 (2.691)		2.620	2.471	2.566
C_2O_1	1.216 (1.227)	1.22	1.234	1.301	1.321 (1.374)
C_2C_3	1.479 (1.455)	1.46	1.457	1.386	1.407 (1.458)
C_3C_4	1.406 (1.401)	1.39	1.404	1.455	1.490 (1.519)
C_4O_5	1.341 (1.355)	1.36	1.358	1.251	1.249 (1.390)
O_5H	0.953 (0.957)	1.04	1.029	1.571	1.688 (1.744)
C_3C_7	1.402 (1.399)	1.41	1.394	1.438	1.391 (1.423)
C_7C_8	1.376 (1.376)		1.365	1.348	1.420 (1.409)
C_8C_9	1.396 (1.396)	1.37	1.384	1.437	1.383 (1.451)
C_9C_{10}	1.376 (1.379)	1.37	1.379	1.349	1.403 (1.450)
C_4C_{10}	1.396 (1.391)	1.41	1.381	1.447	1.421 (1.343)
C_2C_{11}	1.511			1.499	1.494
C_7H	1.072 (1.074)		0.983	1.073	1.072
C_8H	1.072 (1.071)		0.904	1.072	1.072
C_9H	1.073 (1.073)		1.025	1.074	1.072
$C_{10}H$	1.071 (1.070)	1.08	0.986	1.071	1.072
$C_{11}H$	1.078			1.079	1.079
$C_{11}H'(H'')$	1.083			1.083	1.087
			Angles		
O_1O_5H	24.9 (30.2)		21.4	11.8	12.0
$O_1C_2C_3$	121.3 (124.4)	121.0	122.9	121.4	122.3
$C_2C_3C_4$	120.4 (121.5)		120.4	118.3	120.2
$C_3C_4O_5$	123.4 (122.8)		122.7	121.8	119.5
$C_2C_3C_7$	121.3		121.1	122.2	122.5
$C_3C_7C_8$	121.7 (121.1)		121.5	121.3	122.3
$C_7C_8C_9$	119.1 (119.0)		119.4	119.4	120.7
$C_8C_9C_{10}$	120.7 (121.0)		120.5	122.1	119.5
$C_9C_{10}C_4$	120.4 (119.8)		120.5	120.9	121.9
$C_3C_2C_{11}$	119.9			124.8	123.8
C_3C_7H	119.4		117.3	119.1	120.0
C_7C_8H	120.5		117.2	121.1	118.6
C_8C_9H	119.8		117.4	118.4	120.5
$C_9C_{10}H$	121.6		119.0	122.3	121.3
C_4OH	109.4 (114.3)	109.0	106.2	108.1[d]	108.3[e]
$C_2C_{11}H$	108.3			109.2	109.1
$C_2C_{11}H'(H'')$[f]	111.2			111.0	111.7
total energy, au	−457.217 927			−457.189 698	−457.033 987

[a] Data obtained in ref 34b for salicylaldehyde using the 6-31G basis set are reported in parentheses. [b] Microwave structure of salicylaldehyde.[35] [c] Crystal structure of salicylic acid.[36] [d] *o*-Hydroxybenzaldehyde using STO-3G basis set.[34a] [e] Angle C_2O_1H. [f] Dihedral angle $C_3C_2C_{11}H'(H'')$ is approximately 120° in both electronic states.

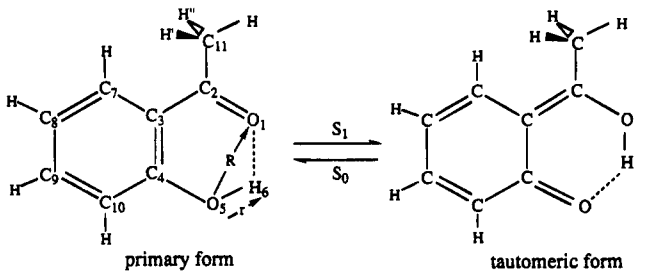

Figure 1. Numbering scheme for atoms and geometric parameters of the O−H···O fragment of the primary and tautomeric forms of *o*-hydroxyacetophenone.

geometry is entirely dissimilar from the zwitterionic structure suggested for the $S_1 \rightarrow S_0$ fluorescing state of methyl salicylate.[42]

The electronic excitation is hence predicted to cause the transfer of the proton and the appearance of the tautomer, which has certain structural features quite different than those of the primary form. Two formal double bonds of the tautomer occur outside the confines of the benzene ring. The associated increase in extent of the π system might be expected to decrease the gap between the HOMO and LUMO. Indeed, the computed excitation energies of the lowest $\pi \rightarrow \pi^*$ transition are 5.6 and 3.9 eV for the ground state primary form and the excited tautomer, respectively. These values can be compared to the experimental transition energies in Table 3 of ref 8. While the CIS calculations overestimate these excitation energies by perhaps 1.5 eV, the calculated Stokes shift of 1.7 eV is in reasonable agreement with the experimental value of 1.3. Turning now to the lowest excited $S_1(n\pi^*)$ state, both tautomers are calculated to lie 5.0 eV above the ground state. While this quantity is unknown for OHAP or other salicylic acid derivatives, it has been measured as 3.4 eV for acetophenone.[43] As in the case of the $\pi-\pi^*$ state, the computed estimate again represents an overestimate of about 1.5 eV. Most importantly, the geometry changes induced by the excited state proton transfer induce small changes in the energy of the $S_1(n\pi^*)$ state. This relative insensitivity appears to be a common feature of similar small aromatic molecules containing a carbonyl group; cf. Table 3.8 in ref 43. The large increase in excitation energy of the $\pi-\pi^*$ state in the geometry of the primary form, compared to the relative insensitivity of $n\pi^*$ to the tautomeric form, leads to the observation that the vertical excitation of smallest energy from the primary form leads to $n\pi^*$, whereas the $\pi-\pi^*$ state is lower for the tautomer. On the other hand, the conclusion that the S_1 state of the tautomer is of $\pi\pi^*$ type does not conform to a deduction from the experimental data.[6]

B. Vibrational Spectrum in the S_0 and S_1 States. The vibrational spectrum of OHAP in both electronic states was computed using the *ab initio* 6-31G basis set, which adds

TABLE 2: Vibrational Frequencies (cm^{-1}) of the Primary Form of OHAP in the S_0 State and the Tautomer in the S_1 State, Obtained Using SCF and CIS Methods, Respectively

		primary form				tautomeric form			
		calc		obs		calc		obs[a]	
no.[b]	sym	freq	major internal coordinates	freq	type[c]	freq	major internal coordinates	freq	type
1	A′	3985	OH	3050[d]	ν(OH)	3605	OH	2300[f]	ν(OH)
2	A′	3406	CH	3088[e]	ν(CH)	3408	CH		
3	A′	3399	CH	3067[e]	ν(CH)	3396	CH		
4	A′	3382	CH	3061[e]	ν(CH)	3384	CH		
5	A′	3366	CH	3040[e]	ν(CH)	3373	CH		
6	A′	3324	CH_3	3030[e]	ν(CH_3)	3310	CH_3		
7	A′	3275	CH_3	3007[e]	ν(CH_3)	3218	CH_3		
8	A′	3207	CH_3	2925[e]	ν(CH_3)	3170	CH_3		
9	A′	1895	CO	1650[g]	ν(CO)	1768	CO/COH	1617[f]	ν(CO)
10	A′	1821	CC/CH	1600[d]	ν(CC) nc[h]	1607	OH/CCH		
11	A′	1774	COH/CH_3/CC			1703	COH/CH/CC		
12	A′	1671	CH_3/CCH/COH			1691	COH/CCH		
13	A′	1634	CH_3/CCH			1646	CH_3/CCH		
14	A′	1626	CH_3			1629	CH_3/OH		
15	A′	1568	CH_3	1440[d]	β(CH_3)	1575	CH_3		
16	A′	1542	COH/CCH	1490[d]	ν(CC)	1541	CH/COH		
17	A′	1458	CC/CCH	1457[d]	ν(CC) nc	1525	CH/COH/CH_3		
18	A′	1437	CCH/CC/CH_3	1360[d]	β(CH_3)	1498	CCH/CC/COH		
19	A′	1391	CCH/COH			1392	CCH/COH	(1414[f])	
20	A′	1342	CCH/COH	1326[g]	β(OH)	1362	CCH/COH	(1300[f])	
21	A′	1289	CCH	1280[d]	β(CH)	1294	CCH		
22	A′	1258	CCH/COH	1221[g]	ν(C−OH)	1196	CCH/COH	1241[f]	ν(C−OH)
23	A′	1201	CH_3/CCH	1170[d]	β(CH)	1173	CH_3/CCH		
24	A′	1140	CCH	1150[d]	β(CH)	1115	CCH		
25	A′	1074	CH_3	1025[d]	β(CH_3)	1069	CH_3/COH		
26	A′	927	CC/CCH/COH			917	CC/CCH/CO		
27	A′	783	skel/COH			741	skel	(801[f])	
28	A′	680	C−COR	706[g]	β(CCC)	739	C−CROH/skel		
29	A′	626	skel/COH	621[g]	β(CCC)	598	skel/CO	(703[f])	
30	A′	524	skel/COH/CH_3			540	C−CROH/skel/CO		
31	A′	467	CCO/COH	480[g]	β(CO)	456	CCO/COH	(423[f])	
32	A′	386	COH/CCOR	434[g]	β(CCC)	399	COH/CCOR	(377[f])	
33	A′	269	CH_3/CCOR/COH	225[g]	β(C−OH)	265	CH_3/CCOR/COH	(269[f])	
34	A″	1640	CH_3	1430[e]	δ(CH_3)	1632	CH_3		
35	A″	1189	CH_3	1046[e]	ϱ(CH_3)	1160	CH_3		
36	A″	1173	CH			1085	CH		
37	A″	1131	CH			1029	CH		
38	A″	1013	CH	970[d]	δ(CH)	931	CH		
39	A″	882	CH	840[d]	δ(CH)	820	CH		
40	A″	858	CH	750[d]	δ(CH) nc	54	CH_3		
41	A″	745	COH			982	COH		
42	A″	674	skel/COH/CH_3	690[d]	δ(CC)	647	skel/CROH/CO		
43	A″	592	skel			558	skel/CH_3		
44	A″	488	skel	452[d]	δ(CC)	509	skel		
45	A″	277	skel/COH	403[d]	δ(CC)	355	skel		
46	A″	183	CH_3	(151[g])		107	CH_3		
47	A″	152	skel/COH	125[g]	C−OH tors	246	skel/COH	(329[f])	
48	A″	81	CCOR	112[g]	C−COR tors	86	CO/COH/skel	(109[f])	

[a] Experimental frequencies of OHAP, for which assignments have not been done, are listed in parentheses. [b] Mode numbers are for the computed spectrum. [c] The following designations are used for expt vibrations: ν, stretching; β, in-plane deformation; δ, out-of-plane deformation; ϱ, rocking. [d] IR spectra of liquid and solid OHAP.[44] [e] IR spectra of acetophenone in the liquid phase.[45] [f] Fluorescence excitation spectra of OHAP in durene mixed crystals at 4.2 K.[8] [g] Fluorescence emission spectra of OHAP in durene mixed crystals at 4.2 K.[8] [h] "nc" indicates no clear-cut correlation was made between atom displacements of the labeled normal coordinate for the excited tautomeric form and atomic displacements of a normal coordinate of the primary form of OHAP.

polarization functions to the O and H atoms involved in the internal H-bond. Although anharmonicity is not included, the calculations are particularly useful in that the proton transfer leads to substantial changes in the structure of the molecule and hence to changes in the spectra. The calculated vibrational spectra are reported in Table 2, where it may be seen that the ground state data agree fairly well with the available experimental information. The frequencies of the in-plane modes unaffected by the H-bond differ from experimental ones by about 12%. The frequency of the OH stretching vibration is ca. 900 cm^{-1} higher than the experimental one. Such a large discrepancy between *ab initio* and observed absolute frequencies is typical for H-bonded systems. For example, the calculated values for tropolone (6-31G basis set) and the formic acid dimer (very large basis set) are 3923[46] and 3705[47] cm^{-1}, respectively, as compared to the corresponding experimental frequencies of 3121[48] and 2688[49] cm^{-1}. Part of the discrepancy is due to neglect of electron correlation, and another error results from use of the harmonic approximation.

Of particular interest here are two in-plane low-frequency modes, namely, 31 and 32. The intramolecular normal coordinate Q_{31} corresponds predominantly to displacements of the atoms in the OH···O chelate ring and can be treated as a nearly pure O···O stretching vibration in terms of the localized OH···O fragment mode.[9] This identification is underscored by the calculated reduced mass for this vibration, which is 8.38 amu,

very close to the value of 8.24 amu for the O···O stretch using eq 2b. Q_{32} also involves the displacements of the atoms in the O−H−O chelate ring as well as the methyl group; the reduced mass of this mode is 4.87 amu. Both of these vibrations are active in the fluorescence spectra of OHAP.[8] Two similar low-frequency in-plane modes have been noted in tropolone,[50] which serves as a model system, containing the symmetric OH···O fragment, in which to study proton transfer in the ground and excited states.

We turn our attention now to the vibrational spectrum of the tautomer in the S_1 state. The OH and CO stretching frequencies are reduced considerably by the changes ensuing from the electronic excitation, while the frequencies of modes which include OH in-plane bending motion change very little. With regard to the vibrations associated with the displacements of H-chelate ring atoms, the vibration located at 1196 cm^{-1} may be assigned to the stretching of the $C_2-O_1H_6$ group, which corresponds to the carbonyl $C_2=O_1$ in the ground state. The vibration at 1768 cm^{-1} can be assigned to the ring carbon−oxygen stretching vibration, which has considerable double-bond character in the excited state. These results agree fairly well with the vibrational assignment of the excitation spectra of OHAP, made in ref 8. Those in-plane modes which are remote from the H-bond are only little affected by the changes ensuing from the electronic excitation. The frequencies of the out-of-plane modes are sensitive to the electronic excitation. In particular, calculations reveal strong increases of modes including OH out-of-plane motion.

Two in-plane low-frequency modes can be identified also in the excited state tautomer structure, the atomic displacements of which show clear correlation with those of Q_{31} and Q_{32} in the S_0 primary form. This result suggests the assignment of two low-frequency vibrations, with frequencies 423 and 377 cm^{-1}, which are very active in the fluorescence excitation spectra of OHAP,[8] as ν_{31} and ν_{32}, respectively. These frequencies are listed in the parentheses in Table 2, which indicate ambiguous experimental assignment.[8] According to our assignment, experimental frequencies of both vibrations are little affected by the $S_1 \leftarrow S_0$ excitation; similar data was obtained for tropolone.[50]

Comparison of the calculated vibrational spectra of OHAP in its S_0 and S_1 states (see columns 3 and 7 in Table 2) shows that the main differences between them occur in the low-frequency region (<1000 cm^{-1}), particularly the out-of-plane vibrations. These results agree fairly well with the available experimental data; cf. Tables 1 and 2 in ref 8. Comparison of the computed vibrational spectra with the available experimental information shows that SCF calculations give a quantitatively correct picture of the ground state (except for the OH stretch mode), while CIS frequencies are only semiquantitatively correct.

In summary, the primary form of OHAP in the ground electronic state and the tautomeric form in the electronically excited state may be considered as different chemical species with regard to certain features of their structure and electronic and vibrational spectra.

C. Correlated 2-D PESs for the S_0 and S_1 Electronic States. As mentioned above, the uncorrelated PES for the S_1 state of OHAP has two distinct minima, in contrast to experiment.[8] Prior work has illustrated a number of occasions where an uncorrelated proton transfer potential, containing two minima, has collapsed to a single well when correlation was added. In order to test whether such is the case here, electron correlation was incorporated into the ground and excited state computations via second-order Moller−Plesset correction to the SCF and CIS

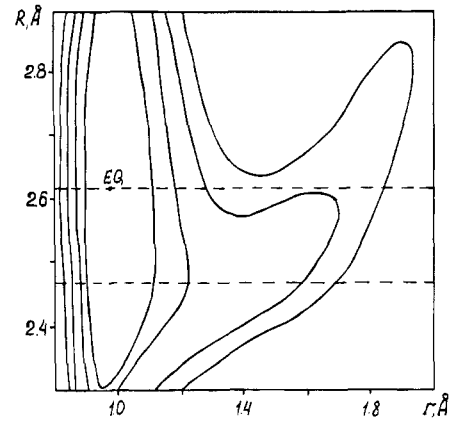

Figure 2. Correlated potential energy surface PES(r,R) for the S_0 state. Contours are in increments of 5 kcal/mol; they are only drawn for energies within 20 kcal/mol of the minimum. EQ represents the equilibrium geometry, with relative energy zero.

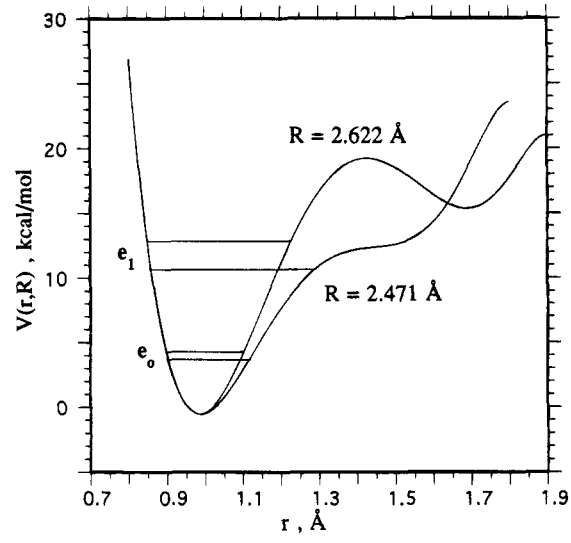

Figure 3. One-dimensional slices through the correlated potential energy surface for the S_0 state for two fixed R values as functions of r, $V(r,R)$; see text. The two lowest lying proton stretch levels are shown for each potential.

energies, respectively. For both electronic states correlation tends to preferentially stabilize the region close to the equilibrium geometry, and this effect is stronger for S_1.

The correlated PES for S_0 is displayed in two-dimensional form in Figure 2. Note that contours are drawn only for regions of the PES where the energy is within 20 kcal/mol of the equilibrium structure. Consider the shape of one-dimensional slices through the PES for fixed R as functions of r, $V(r,R)$, at two different values of R. These functions are used in the present paper as the potentials for proton (deuteron) stretches; see eq 6. At the equilibrium O···O distance, R_e, the $V(r,R_e)$ function has two inequivalent minima (Figure 3), where the left (deepest) minimum corresponds to the primary form and the right (highest) to the tautomeric form, in which the proton is connected to the former carbonyl oxygen; see Figure 1. At a shorter O···O distances, e.g. 2.471 Å, which corresponds to the equilibrium R(O···O) distance of the tautomer, the local minimum disappears and $V(r,R)$ has only a shoulder at $r \sim 1.4$ Å.

Like S_0, the correlated PES of S_1 has only one minimum. But this minimum differs from S_0 in that it corresponds to the tautomer, in harmony with the available experimental data.[8] One way to compare the PESs of the two electronic states is to consider the shapes of the one-dimensional slices $V^*(r,R)$ (where the asterisk represents the excited state) at the same values of

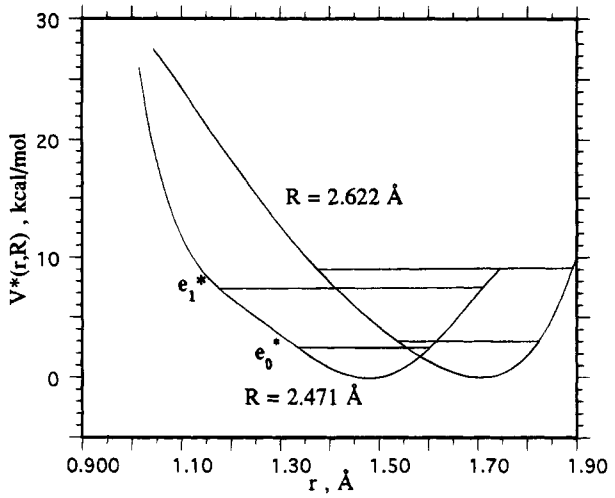

Figure 4. One-dimensional slices through the correlated potential energy surface for the S_1 state for two fixed R values as functions of r, $V^*(r,R)$; see text. The two lowest lying proton stretch levels are shown for each potential.

TABLE 3: Relative Energies and Frequencies (cm^{-1}) in S_0 and S_1 States, Obtained with the Correlated PESs (Experimental Data Are Reported in Parentheses)

quantum nos.		S_0 relative energy, E_{vn}		S_1 relative energy, E^*_{vn}	
v	n	H	D	H	D
0	0	0	0	0	0
0	1	360 (480[a])	338	498 (423[a])	476
0	2	715	665	991	952
0	3	1072	991	1482	
1	0	2765 (3050[b])	2185 (2280–2350[c])	1564 (2300[a])	1220

[a] Expt data from ref 8. [b] Expt data from ref 44. [c] Expt data from ref 53.

R as in the ground electronic state; cf. Figures 3 and 4. In contrast to S_0, the $V^*(r,R)$ function has only one minimum at its equilibrium O···O distance.

The vibrational frequencies of the O···O and OH stretches in both electronic states were calculated, along with the H/D isotope effects on these frequencies, using the adiabatic approximation (see Methods of Calculation B). After solving the Schrödinger equation (8) for O···O stretching vibrations, we obtain the eigenvalues E_{vn} which depend on two quantum numbers. The frequency of the O···O stretching vibration is associated with the energy difference

$$\nu(\text{O}\cdots\text{O}) = E_{01} - E_{00} \tag{9}$$

while that of the OH (OD) stretch can be written as

$$\nu(\text{OH}) = E_{10} - E_{00} \tag{10}$$

Energy levels E_{vn} calculated for the S_0 state are reported in Table 3, along with the frequencies. The calculated OH (OD) stretching frequencies differ from experiment by less than 20%. It is underscored that this treatment of OH (OD) stretch provides superior agreement with experiment, by several hundred cm^{-1}, compared to a harmonic approximation of the entire molecule, as in Table 2, which yields a stretching frequency of 3985 cm^{-1}. The O···O stretching frequency for H (360 cm^{-1}) is a little higher than for D (338 cm^{-1}), while it is ca. 25% larger than experiment for the OH species.

The insensitivity of ν to n, as evidenced by the uniform spacing of the energies in the first few rows of Table 3, suggests that the O···O stretching vibration can be treated as approximately harmonic in the ground electronic state for small n.[8] A similar result was obtained in experiments by Sekiya et al.[50] for tropolone. Analogous data for the S_1 state may be seen in Table 3 to reproduce some experimental trends, established for $S_1 \leftarrow S_0$ excitation in OHAP:[8] (1) lowered OH stretching frequency in S_1; (2) little change in the O···O stretching frequency as n increases, indicating this vibration can be treated approximately as harmonic in S_1 for small n. A similar result was obtained in experiments by Sekiya et al.[50] for tropolone and Fuke et al.[54] for azaindole dimer.

The absolute value of the OH stretching frequency is smaller by ~32% than the experimental value. In contrast to experiment, our calculations predict an increase of O···O stretching frequency upon electronic excitation. This discrepancy is likely associated with errors in the calculated excited state PES.

The H/D isotopic ratio of the OH stretch was computed to be 1.27 in the ground electronic state (cf. experimental value of 1.33) and ca. 1.28 in S_1. Since the PES of each electronic state has only a single minimum, there is no reason to expect anomalous isotopic effects.

In summary, the correlated PES for the S_0 state of OHAP has quantitatively correct character, while that of the S_1 state is less true to experimental observation.

Discussion

It is stressed first that excitation to the lowest excited singlet state of OHAP is found by the calculations to lead to the transfer of the proton from one oxygen atom to its partner in the H-bond. The PES in each state contains only a single minimum. The transfer is accompanied by large changes in the geometric parameters of the H-chelate ring as well as minor distortion of the benzene skeleton. In contrast to our results, Nagaoka and Nagashima[1] suggested the process of producing the fluorescence state in a molecule closely related to OHAP, *o*-hydroxybenzaldehyde (OHBA), might not be the PT at all, but rather isomerization from the primary conformer to some other which is characterized by strong distortion of the benzene skeleton but leaves the bridging proton near the hydroxyl oxygen. Their contention is supported in part by calculations of the OHBA structure in the ground and lowest excited states that have been published recently. Using CASSCF techniques with an STO-3G basis set, Sobolewski and Domcke[34a] obtained the geometrical parameters for the tautomeric form of OHBA reported in the parentheses in Table 1. Comparison of the last two columns shows that the geometry of the tautomeric form obtained for the excited state of OHBA, while it does indicate the proton has been transferred across to the carbonyl oxygen, differs in certain important respects from our findings with OHAP. Whereas the loss of the proton induces a reduction of 0.1 Å of the former C_4O_5 carbonyl bond for OHAP, the STO-3G results of Sobolewski and Domcke[34a] indicate no appreciable change in bond length. There are discrepancies within the benzene ring as well. Both the C_3C_7 and C_8C_9 bonds of OHAP are shortened by the proton transfer, as compared to lengthening in OHBA; opposite trends are observed for C_4C_{10} as well.

Of particular interest are the aspects of the H-bond geometry. According to Sobolewski and Domcke,[34a] the proton transfer has little effect upon the H-bond length. This conclusion conflicts with experiment,[8] according to which electron excitation of OHAP and related molecules results in shortening of the O···O distance (strong decrease of the OH stretch frequency; presence of low-frequency mode progressions, associated with the O···O stretching vibrations). The anomalously long C_4O_5 carbonyl bond computed by these workers disagrees with the appearance of a "ring carbon–oxygen stretching vibration,

which has a considerable double-bond character in the excited state".[8] Some of the discrepancy with experimental observations of the calculations reported in refs 1 and 34a may be due to the use of a minimal basis set. Indeed, the bond lengths obtained for the ground state of OHBA by Sobolewski and Domcke[34a] are in poor agreement with experimental data, especially the geometrical parameters of the H-chelate ring. The calculated[34a] C_2C_3 and C_4O_5 bond lengths are particularly bad.

As noted earlier, the lowest energy vertical excitation from the S_0 OHAP equilibrium geometry (the primary form) was calculated to be of $n \rightarrow \pi^*$ type, while the vertical excitation from the tautomer geometry is $\pi \rightarrow \pi^*$. The ESPT process in OHAP can hence be associated with vibrational relaxation, during which the molecule passes from the $S_1(n\pi^*)$ state to $S_1(\pi\pi^*)$. These results imply that radiationless processes may play an important role in the lowest excited singlet state dynamics of OHAP, consonant with experimental data wherein the nonradiative processes dominate over the transfer processes,[55] resulting in a very small fluorescence quantum yield of OHAP.[56] It should be noted that similar energies of the $S_1(n\pi^*)$ and $S_1(\pi\pi^*)$ states are typical of salicylic acid derivatives; see for example Figure 2 in ref 34a.

Comparison of the computed energies of vertical excitation of the present paper with those in ref 34a shows the advantage of multiconfiguration techniques to compute the absolute magnitudes of these properties. While the CAS calculations reproduce these vertical energies rather well (Table 1 in ref 34a), CIS is less successful in this regard (see Results A).

Theoretical one- and two-dimensional potentials for the S_0 and S_1 states of aromatic molecules with an asymmetric OH···O fragment have been obtained for salicylic acid,[57] some of its derivatives,[58] and *o*-hydroxyflavone[59] using semiempirical quantum mechanical methods. Catalan et al.[57] and Orttung et al.[58a] concluded that the lowest excited singlet state potential may contain two inequivalent minima, corresponding to the primary and tautomeric structures (although this result may have been forced by the use of a frozen long interoxygen distance[57]). This result contrasts with those reported here and the single-well *ab initio* potentials of Sobolewski and Domcke.[34a] The appearance of the second well in the earlier works is likely caused by use of approximate semiempirical methods. According to our calculations, electron correlation plays a crucial role in these systems. Indeed, the uncorrelated PES in the S_1 state of OHAP was found to possess two minima, with the relative energy of the primary excited state only 0.8 kcal/mol higher than the tautomer. In contrast, the correlated PESs of OHAP in both electronic states were found to contain a single minimum. The shapes of these PESs are verified by the calculated vibrational frequencies of the O···O and OH (OD) stretch.

It is worthwhile, finally, to discuss terminology issues connected with the intramolecular ESPT phenomenon. In the literature devoted to ESPT in H-bonded systems, hydrogen atom transfer is occasionally used synonymously with proton transfer; see for example ref 60. It is our opinion that the ESPT process is not as well described as a hydrogen atom transfer.

In terms of the "localized fragment" model the gas phase proton transfer can be presented as

$$A{:}H + {:}B \rightarrow (A{:}H{:}B) \rightarrow A{:}^- + {}^+H{:}B \qquad (11a)$$

or

$$(A{:}H)^+ + {:}B \rightarrow (A{:}H{:}B)^+ \rightarrow A{:} + (H{:}B)^+ \qquad (11b)$$

where (A:H:B) and $(A:H:B)^+$ refer to neutral and ionic H-bonded complexes, respectively, which are usually quite stable. The gas phase hydrogen atom transfer, in contrast, can be represented as

$$A{:}H + {\cdot}B \rightarrow (A{:}H{\cdot}B) \rightarrow A{\cdot} + H{:}B \qquad (12)$$

where (A:H·B) is an "encounter complex", which is not usually very stable. Intramolecular ESPT is described much better by equations 11.

Conclusions

The correlated PES of the two lowest singlet states of OHAP each have a single minimum, corresponding to the primary form in the ground state and the proton-transferred tautomer in S_1. Excited state proton transfer causes large changes in the geometry of the H-chelate ring, with more minor perturbations in the benzene ring. The different tautomeric forms of the ground and excited states may be regarded as different molecules, with regard to many of their physical and chemical properties. In particular, the vibrational spectrum of S_1 OHAP is quite different from that of the ground state, especially in the low-frequency region. The fluorescent state of OHAP is of $S_1(\pi\pi^*)$ type, whereas vertical excitation directly from the equilibrium S_0 geometry is of $n\pi^*$ type. The entire ESPT process may hence be considered as vibrational relaxation, accompanied by the proton motion and $S_1(n\pi^*) \rightarrow S_1(\pi\pi^*)$ transition.

Acknowledgment. We thank Professor N. D. Sokolov for a critical reading of the manuscript and for valuable discussions. This work was supported by the U.S. National Science Foundation (CHE-9123824) and by the CAST Program of the National Research Council.

References and Notes

(1) Nagaoka, S.; Nagashima, U. *Chem. Phys.* **1988**, *136*, 153 and references therein.
(2) Douhal, A.; Lahmani, F.; Zehnacker-Rentien, A. *Chem. Phys.* **1993**, *178*, 493.
(3) Pant, D. D.; Joshi, H. C.; Bisht, P. B.; Tripathi, H. B. *Chem. Phys.* **1994**, *185*, 137.
(4) Acuna, A. U.; Amat-Guerri, F.; Catalan, J.; Gonzalez-Tables, F. *J. Phys. Chem.* **1980**, *84*, 629.
(5) Morgan, M. A.; Orton, E.; Pimentel, G. S. *J. Phys. Chem.* **1990**, *94*, 7927.
(6) Orton, E.; Morgan, M. A.; Pimentel, G. S. *J. Phys. Chem.* **1990**, *94*, 7936.
(7) Nagaoka, S.; Nagashima, U.; Ohta, N.; Fujita, M.; Takemura, T. *J. Phys. Chem.* **1988**, *92*, 166.
(8) Nishiya, T.; Yamauchi, S.; Hirota, N.; Baba, M.; Hanazaki, I. *J. Phys. Chem.* **1986**, *90*, 5730.
(9) Stepanov, B. I. *Zh. Fiz. Khim.* **1945**, *19*, 507; **1946**, *20*, 907.
(10) Foresman, J. B.; Head-Gordon, M.; Pople, J. A.; Frish, M. J. *J. Phys. Chem.* **1992**, *96*, 135.
(11) *Gaussian 92*, Revision A; Frish, M. J., Trucks, G. W., Head-Gordon, M., Gill, P. M. W., Wong, M. W., Foresman, J. B., Johnson, B. G., Shclegel, H. B., Robb, M. A., Replogle, E. S., Comperts, R., Andres, J. L., Raghavachari, K., Binkley, J. S., Gonzalez, C., Martin, R. L., Fox, D. J., Defrees, D. J., Baker, J., Stewart, J. J. P., Pople, J. A., Eds.; Gaussian, Inc.: Pittsburgh, PA, 1992.
(12) Hehre, W. J.; Radom, L.; Schleyer, P. v. R.; Pople, J. A. *Ab initio Molecular Orbital Theory*; Wiley: New York, 1986.
(13) Carrington, T.; Miller, W. H. *J. Chem. Phys.* **1986**, *84*, 4364.
(14) Shida, N.; Barbara, P. F.; Almlöf, J. *J. Chem. Phys.* **1989**, *91*, 4061.
(15) Vener, M. V.; Scheiner, S.; Sokolov, N. D. Submitted for publication.
(16) Laermer, F.; Elsaesser, T.; Kaiser, W. *Chem. Phys. Lett.* **1988**, *148*, 119.
(17) Herek, J. L.; Pedersen, S.; Banares, L.; Zewail, A. H. *J. Chem. Phys.* **1992**, *97*, 9046.
(18) Singh, T. R.; Wood, J. L. *J. Chem. Phys.* **1968**, *48*, 4567.
(19) Sokolov, N. D.; Savel'ev, V. A. *Chem. Phys.* **1977**, *22*, 383.
(20) Barton, S. A.; Thorson, W. R. *J. Chem. Phys.* **1979**, *71*, 4263.

(21) Thi-Ding, Q.; Xing-Guo, Z.; Xing-Wen, L.; Kono, H.; Lin, S. H. *Mol. Phys.* **1982**, *47*, 713.
(22) Manz, J.; Meyer, R.; Romelt, J. *Chem. Phys. Lett.* **1983**, *96*, 607.
(23) Ezra, G. S. *Chem. Phys. Lett.* **1983**, *101*, 259.
(24) Johnson, B. R.; Skodje, R. T.; Reinhard, W. P. *Chem. Phys. Lett.* **1984**, *112*, 396.
(25) Manz, J.; Meyer, R.; Pollak, E.; Romelt, J.; Schor, H. H. R. *Chem. Phys.* **1984**, *83*, 333.
(26) Sage, M. R. *Chem. Phys. Lett.* **1985**, *93*, 453.
(27) Kubash, C.; Nguyen Vien, G.; Richard-Viard, M. *J. Chem. Phys.* **1991**, *94*, 1929.
(28) Grace, B.; Skodje, R. T. *J. Chem. Phys.* **1991**, *95*, 7249.
(29) Sokolov, N. D.; Vener, M. V. *Chem. Phys.* **1992**, *168*, 29.
(30) Sato, N.; Iwata, S. *J. Chem. Phys.* **1988**, *89*, 2932.
(31) Sokolov, N. D.; Vener, M. V.; Savel'ev, V. A. *J. Mol. Struct.* **1990**, *222*, 365.
(32) Sokolov, N. D.; Vener, M. V.; Savel'ev, V. A. *J. Mol. Struct.* **1988**, *177*, 93.
(33) Johnson, B. R. *J. Chem. Phys.* **1977**, *67*, 4086.
(34) (a) Sobolewski, A. L.; Domcke, W. *Chem. Phys.* **1994**, *184*, 115. (b) George, P.; Bock, C. W.; Trachtman, M. *J. Mol. Struct. (THEOCHEM)* **1985**, *133*, 11.
(35) Jones, H.; Curl, R. F., Jr. *J. Mol. Struct.* **1972**, *42*, 65.
(36) Sundralingham, M.; Jensen, J. M. *Acta Crystallogr.* **1965**, *18B*, 1053.
(37) Dick, B. *J. Phys. Chem.* **1990**, *94*, 5752.
(38) Ersting, N. P.; Arthen-Engeland, Th.; Rodriquez, M. A.; Thiel, W. *J. Chem. Phys.* **1992**, *97*, 3914.
(39) Tanaka, H.; Nihimoto, K. *J. Phys. Chem.* **1984**, *88*, 1052.
(40) Duan, X.; Scheiner, S. *Chem. Phys. Lett.* **1993**, *204*, 36.
(41) Klopffer, W. *Adv. Photochem.* **1977**, *10*, 311.
(42) Smith, K. K.; Kaufmann, K. J. *J. Phys. Chem.* **1981**, *85*, 2895.
(43) McGlynn, S. P.; Azumi, T.; Kinoshita, M. *Molecular spectroscopy of the triplet state*. Prentice-Hall: New Jersey, 1969.
(44) Gupta, V. P.; Gupta, D.; Jain, S. M. *Int. J. Pure Appl. Phys.* **1976**, *14*, 846.
(45) Gambi, A.; Giorgianni, S.; Passerini, A.; Visinoni, R.; Ghersetti, S. *Spectrochim. Acta* **1980**, *36A*, 871.
(46) Redington, R. L.; Bock, C. W. *J. Phys. Chem.* **1991**, *95*, 10284.
(47) Shida, N.; Barbara, P. F.; Almlöf, J. *J. Chem. Phys.* **1991**, *94*, 3663.
(48) Redington, R. L.; Redington, T. E. *J. Mol. Spectrosc.* **1979**, *78*, 229.
(49) Bertie, J. E.; Michallian, K. H. *J. Chem. Phys.* **1982**, *76*, 886.
(50) Sekiya, H.; Nagashima, Y.; Tsuji, T.; Nishimura, Y.; Mori, A.; Takeshita, H. *J. Phys. Chem.* **1991**, *95*, 10311.
(51) Frish, M. J.; Scheiner, A. C.; Schaefer, H. F., III. *J. Chem. Phys.* **1985**, *82*, 4194.
(52) Luth, K.; Scheiner, S. *J. Phys. Chem.* **1994**, *98*, 3582.
(53) Petenau, L. A.; Mathies, R. A. *J. Phys. Chem.* **1992**, *96*, 6910.
(54) Fuke, K.; Kaya, K. *J. Phys. Chem.* **1989**, *93*, 614.
(55) Nagaoka, S.; Hirota, N.; Sumitani, M.; Yoshihara, K. *J. Am. Chem. Soc.* **1983**, *105*, 4220.
(56) Catalan, J.; Toribio, F.; Acuna, A. U. *J. Phys. Chem.* **1982**, *86*, 303.
(57) Catalan, J.; Fernandez-Alonso, J. I. *J. Mol. Struct.* **1975**, *27*, 59.
(58) (a) Orttung, W. H.; Scott, G. W.; Vosooghi, D. *J. Mol. Struct. (THEOCHEM)* **1984**, *109*, 161. (b) Sanchez-Cabezudo, M.; De Paz, J. L. G.; Catalán, J.; Amat-Guerri, F. *J. Mol. Struct.* **1985**, *131*, 277.
(59) Muhlpfordt, A.; Bultmann, T.; Ernsting, N. P.; Dick, B. *Chem. Phys.* **1994**, *181*, 447.
(60) Barbara, P. F.; Walch, P. K.; Brus, L. E. *J. Phys. Chem.* **1989**, *93*, 29.

JP942152K